Modulation of age-related insulin sensitivity by VEGF-dependent vascular plasticity in adipose tissues

Jennifer Honek[a], Takahiro Seki[a], Hideki Iwamoto[a], Carina Fischer[a], Jingrong Li[b], Sharon Lim[a], Nilesh J. Samani[c], Jingwu Zang[b], and Yihai Cao[a,c,d,1]

[a]Department of Microbiology, Tumor and Cell Biology, Karolinska Institute, 171 77 Stockholm, Sweden; [b]Simcere Pharmaceutical Research and Development, Nanjing, Jiangsu 210042, China; [c]Department of Cardiovascular Sciences, University of Leicester and National Institute for Health Research Leicester Cardiovascular Biomedical Research Unit, Glenfield Hospital, Leicester LE3 9QP, United Kingdom; and [d]Department of Medicine and Health Sciences, Linköping University, 581 83 Linköping, Sweden

Edited by Tadamitsu Kishimoto, Immunology Frontier Research Center, Osaka University, Suita, Japan, and approved September 10, 2014 (received for review August 19, 2014)

Mechanisms underlying age-related obesity and insulin resistance are generally unknown. Here, we report age-related adipose vascular changes markedly modulated fat mass, adipocyte functions, blood lipid composition, and insulin sensitivity. Notably, VEGF expression levels in various white adipose tissues (WATs) underwent changes uninterruptedly in different age populations. Anti-VEGF and anti-VEGF receptor 2 treatment in different age populations showed marked variations of vascular regression, with midaged mice exhibiting modest sensitivity. Interestingly, anti-VEGF treatment produced opposing effects on WAT adipocyte sizes in different age populations and affected vascular density and adipocyte sizes in brown adipose tissue. Consistent with changes of vasculatures and adipocyte sizes, anti-VEGF treatment increased insulin sensitivity in young and old mice but had no effects in the midaged group. Surprisingly, anti-VEGF treatment significantly improved insulin sensitivity in midaged obese mice fed a high-fat diet. Our findings demonstrate that adipose vasculatures show differential responses to anti-VEGF treatment in various age populations and have therapeutic implications for treatment of obesity and diabetes with anti-VEGF-based antiangiogenic drugs.

angiogenesis | aging | endothelial cells | metabolic disorders | vascularization

Overweight and obesity are global pandemic predisease syndromes that affect a majority of people during their lifetime. Even those who are lean for the time being might have to change their lifestyles to prevent future development of obesity and related disorders, including type 2 diabetes, cardiovascular disease, hypertension, and certain types of malignant disease. It is known that humans and animals at a certain age are more vulnerable to develop obesity. Midaged and elderly populations tend to be more susceptible than younger populations to developing insulin resistance and type 2 diabetes (1). Despite this notion, mechanisms underlying age-related development of obesity and type 2 diabetes are unknown.

Current approaches of understanding obesity and diabetes development focus on studying adipocytes per se or adipose-associated inflammatory cells (2–4). However, the role of vascular networks, as one of the most dominant nonadipocyte components in all adipose tissues, in modulation of adipocyte functions is poorly understood. White adipose tissue (WAT) and brown adipose tissue (BAT) are hypervascularized and capillary networks form a "honeycomb-like" structure in which each adipocyte is embedded in a vascular chamber (5–7). The anatomical proximity and intimate interaction between adipocytes and capillaries suggest that microvasculatures are crucial for modulation of adipocyte functions under physiological and pathological conditions. Because adipose tissues undergo expansion and shrinkage during the entire adulthood, adipose vasculatures have to exhibit the same magnitude of plasticity to cope with adipose tissue mass and functional changes. Blood vessels not only provide nutrients and oxygen for adipocytes, cells in the vessel wall are also an important source of stem cells that can differentiate into preadipocytes and adipocytes, and adjust the adipose tissue mass depending on metabolic demands (6, 8–10).

To sustain vessel numbers, vascular integrity, and architectures, adipocytes, together with other cell types including inflammatory cells and mesenchymal cells, produce a variety of soluble and nonsoluble factors, cytokines, and adipokines to modulate vascular functions through a paracrine mechanism (7). Among all known vascular factors, VEGF is the most prominently expressed angiogenic factor in adipose tissues and significantly modulates adipose angiogenesis and functions under physiological and pathological conditions (11, 12). VEGF binds to VEGF receptor 1 (VEGFR1) and VEGF receptor 2 (VEGFR2), two tyrosine kinase receptors, primarily expressed in endothelial cells (13, 14). Although VEGFR2-mediated signaling has been associated with VEGF-induced angiogenesis, vascular permeability, and other vasculature-related functions, the functional consequences of the VEGFR1-triggered signaling remain enigmatic. VEGF is also an important vascular survival factor that prevents endothelial cell apoptosis (15). Based on its prominent functions under pathological conditions, antiangiogenic drugs targeting the VEGF–VEGFR2 signaling pathway have been developed for treatment of cancer and ophthalmological disease (16–18).

In this paper, we present our findings of age-related vascular changes in adipose tissues and define VEGF as a key factor for maintenance of adipose vascular integrity. Importantly, age-related differential responses of adipose vasculature to anti-VEGF drugs

Significance

The etiology and mechanisms underlying the age-related high incidence of metabolic diseases such as type 2 diabetes are not fully understood. In this paper, we show that blood vasculatures in the adipose tissues experience continuous changes during aging and VEGF is a key angiogenic factor controlling microvessel numbers and functions. Surprisingly, targeting VEGF and VEGF receptor 2 by specific blocking drugs produces different and sometimes opposing effects on white adipocytes, resulting in marked differences in insulin sensitivity in different age groups. These findings demonstrate that vascular changes in white adipose tissues are the key determinant for modulation of adipocyte metabolism and insulin sensitivity and provide valuable information for treatment of obesity and diabetes by targeting the vasculature.

Author contributions: Y.C. designed research; J.H., T.S., H.I., and C.F. performed research; J.L., N.J.S., and J.Z. contributed new reagents/analytic tools; J.H., T.S., H.I., C.F., S.L., and Y.C. analyzed data; and J.H. and Y.C. wrote the paper.

The authors declare no conflict of interest.

This article is a PNAS Direct Submission.

[1]To whom correspondence should be addressed. Email: yihai.cao@ki.se.

This article contains supporting information online at www.pnas.org/lookup/suppl/doi:10.1073/pnas.1415825111/-/DCSupplemental.

resulted in a significant difference of insulin sensitivity in various age populations. These findings demonstrate that adipose VEGF levels and vascularization are key determinants for modulation of metabolism and insulin sensitivity. Our data also provide information in understanding the role of adipose vasculature in development of obesity and diabetes. Based on our compelling evidence, it is reasonable to speculate that there may be differential responses of metabolic changes in human populations of different ages to clinically available antiangiogenic drugs.

Results

Changes of WAT Vasculatures and Adipocyte Sizes During Aging. To study the impact of age on vascularization in adipose tissues, we chose C57BL/6 syngeneic mice at different ages for our studies. If the mouse lifespan of approximate 2 y is converted to human lifetime of 100 y, one mouse day is approximately equal to 50 human days. To cover the lifetime, we chose 1-, 4-, 10-, 12-, and 16-mo-old mice, which are equivalent to 4-, 17-, 42-, 50-, and 70-y-old humans. In C57BL/6 mice, body weight and body mass index (BMI) increased from 1 to 10 mo of age and stabilized after 10 mo (Fig. 1*A*). Similarly, average adipocyte size in subcutaneous (s.c.) and epididymal WAT (sc- and epiWAT) significantly increased during the age of 1–10 mo (Fig. 1 *B* and *C* and Fig. S1 *A* and *B*). However, scWAT and epiWAT adipocytes reached their maximal average sizes at the age of 10 mo and became successively decreased thereafter (Fig. 1 *B* and *C* and Fig. S1 *A* and *B*). In contrast to alterations of adipocyte size, microvessel density and numbers in scWAT and epiWAT markedly decreased during aging, with the highest density at 1 mo and lowest at 10 mo of age (Fig. 1 *B–E* and Fig. S1 *A* and *C*). After 10 mo, epiWAT microvessel density gradually increased, and a considerable increase was detected at the age of 16 mo (Fig. S1 *A* and *C*). Despite changes of vessel density, pericyte coverage in adipose vasculatures of all studied age groups was similar (Fig. S1 *D–H*).

Vascular and Adipocyte Changes in BAT. We next analyzed adipocytes and microvessels in BAT of different age populations. Surprisingly, total mass of interscapular BAT (intBAT) increased during aging (Fig. 2*B*). Average adipocyte size significantly increased during aging and reached a maximum at 12 mo (Fig. 2 *A* and *C*). It seemed that lipid droplet content increased during aging and large lipid droplets were detectable in the 10- and 12-mo groups (Fig. 2*A*). Microvessel numbers per adipocyte significantly decreased during aging despite the increase of intBAT mass (Fig. 2 *B* and *D*). When total vascular density was assessed, a significant decrease of intBAT vascularization was found at the age of 10 mo, followed by a marked increase thereafter (Fig. 2 *A* and *D*). To correlate these findings with intBAT activation, we measured the expression of uncoupling protein 1 (UCP1), a key component of the mitochondrial machinery, which generates heat by nonshivering thermogenesis. Surprisingly, the highest UCP1 level in intBAT was detected at the age of 4 mo (Fig. 2 *A* and *E*). This is an unexpected finding because it has been speculated that BAT activation occurred in newborns and younger ages. After 4 mo, intBAT *Ucp1* expression decreased (Fig. 2*E*). These findings show that adipocytes, vascular density, and intBAT activation undergo marked changes during aging.

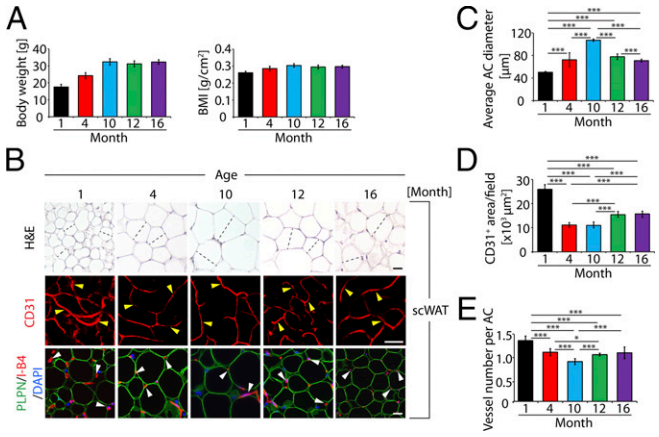

Fig. 1. Age-related changes of adipose vasculature and scWAT adipocyte size. (*A*) Body weight and BMI of 1-, 4-, 10-, 12-, and 16-mo-old mice (n = 10–12). (*B*) Histology of adipocytes and vascular density of scWAT. scWATs were stained with H&E, CD31 (red), or perilipin (PLPN, green) plus isolectin B4 (I-B4, red) counterstained with DAPI (blue) nucleus staining. Arrowheads point to microvessels. Dashed lines show diameters of typical adipocytes. (Scale bars, 50 μm.) (*C*) Average diameters of adipocytes of scWAT. Adipocyte sizes were quantified from 120 adipocytes from 12 fields. (*D*) Quantification of total microvessel density in scWAT (12 fields per group). (*E*) Quantification of microvessel numbers per adipocyte in scWAT (total numbers of microvessels were divided by total numbers of adipocytes per field; 12 fields per group). $^{*}P < 0.05$, $^{***}P < 0.001$.

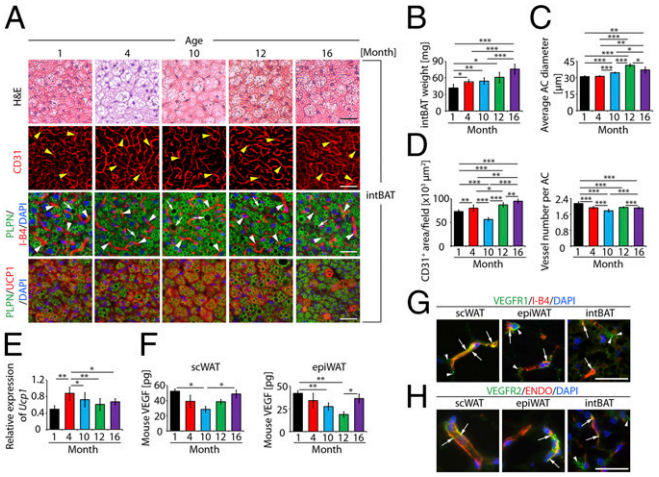

Fig. 2. Age-related changes of adipose vasculature and intBAT adipocyte size. (*A*) Histology of intBAT adipocytes and vascular density. intBAT was stained with H&E, CD31 (red), or PLPN (green) plus I-B4 (red) with DAPI nucleus staining (blue). UCP1 (red), PLPN (green) and DAPI (blue) triple staining is shown in lowest panels. Arrowheads point to microvessels and arrows point to lipid droplets. (Scale bars, 50 μm.) (*B*) Total weight of intBAT of 1-, 4-, 10-, 12-, and 16-mo-old mice (n = 10–12). (*C*) Average diameters of intBAT adipocytes. Adipocyte sizes were quantified from 120 adipocytes from 12 fields. (*D*) Quantification of total vascular density and microvessel numbers per adipocyte in intBAT (12 fields per group). (*E*) Quantification of *Ucp1* mRNA expression by qPCR (six samples in duplicates per group). (*F*) Quantification of VEGF protein levels in scWAT and epiWAT of different age groups (four samples in duplicates per group). (*G*) Colocalization of VEGFR1 protein expression with a specific anti-VEGFR1 antibody with I-B4 in scWAT, epiWAT, and intBAT. Arrows indicate VEGFR1 and I-B4 double-positive signals. Arrowheads point to nonoverlapping signals. (Scale bar, 50 μm.) (*H*) Colocalization of VEGFR2 protein expression with a specific anti-VEGFR2 antibody with endomucin (ENDO) in scWAT, epiWAT, and intBAT of 1-mo-old mice. Arrows indicate VEGFR2 and ENDO double-positive signals. Arrowheads point to nonoverlapping signals. (Scale bar, 50μm.) $^{*}P < 0.05$, $^{**}P < 0.01$, $^{***}P < 0.001$.

Age-Related Differential VEGF Expression and Anti-VEGF Responses in WAT and BAT. To gain molecular information underlying age-related adipose vascular changes, VEGF expression was analyzed. Interestingly, VEGF protein levels in scWAT and epiWAT exhibited a pattern similar to that of vascular density in different age groups. Highest VEGF levels were detected in 1-mo-old mice and 10- and 12-mo groups showed the lowest levels (Fig. 2*F*). Importantly, VEGF levels in scWAT and epiWAT were increased

MEDICAL SCIENCES

in the 16-mo group. VEGF expression correlated with age-related changes of vascular density in these depots, suggesting that VEGF could be the primary angiogenic factor responsible for maintenance of adipose vasculature. We measured *Vegfr1* and *Vegfr2* expression by quantitative PCR (qPCR). *Vegfr1* expression levels in scWAT and epiWAT exhibited a similar pattern with significant increases of *Vegfr1* expression in the 10-mo group, followed by sharp decreases in 12- and 16-mo groups (Fig. S2*A*). These findings reconcile with the general functions of VEGFR1, which is likely to act as a negative receptor in the modulation of angiogenesis. Indeed, microvessel densities of scWAT and epiWAT were significantly lower in the 10-mo group compared with other age groups (Fig. 1 *B*, *D*, and *E* and Fig. S1 *A* and *C*). In contrast, *Vegfr2* expression was decreased along aging in scWAT (Fig. S2*B*). However, the decrease of *Vegfr2* expression in epiWAT was not as overwhelming as in scWAT (Fig. S2*B*). Notably, *Vegfr1* and *Vegfr2* expression in intBAT exhibited a similar pattern with a significant decrease of receptor expression in the 12-mo group, followed by a marked increase in the 16-mo group (Fig. S2 *A* and *B*). The underlying mechanism by which *Vegfr1* and *Vegfr2* expression was increased in 16-mo intBAT remains to be elucidated.

We next localized VEGFR1 and VEGFR2 expression in various adipose depots. Although VEGFR1 was also expressed in microvessels of scWAT, epiWAT, and intBAT, its expression pattern was rather diffused (Fig. 2*G*), indicating nonendothelial expression of this receptor. VEGFR2 expression was relatively restricted to microvessels in scWAT and epiWAT (Fig. 2*H*). Less-abundant VEGFR2 expression was detected in intBAT.

To provide further evidence of VEGF-associated vascular functions in adipose tissues we took a pharmacological approach to block VEGF functions using an anti-mouse VEGF neutralizing antibody (anti-VEGF treatment). This treatment has previously been shown to block angiogenesis in mouse tumor models and in healthy tissues (19, 20). Anti-VEGF treatment induced vascular regression in scWAT and epiWAT in all groups (Fig. 3*A* and Fig. S2*C*). These findings provide evidence that VEGF is a key survival factor for adipose vasculatures. Despite effects of anti-VEGF treatment on adipose vasculatures, the VEGF-dependent vascular integrity in scWAT and epiWAT varied considerably among different age groups. In the 1-mo group, more than 60% of scWAT microvessels were regressed after only 4 wk of anti-VEGF-treatment (Fig. 3 *A* and *E*). A similar regressive effect was also found in 1-mo epiWAT in response to anti-VEGF treatment (Fig. S2 *C* and *F*). Unlike younger mice, the midaged (7-mo-old) group showed intrinsic resistance to anti-VEGF treatment and only modest vascular regression was detected (Fig. 3 *A* and *E* and Fig. S2 *C* and *F*). Notably, epiWAT of 7-mo-old mice showed minimal response (8%) in vascular reduction compared with that of 1-mo-old mice (greater than sixfold difference in sensitivity). These data demonstrate that differential vascular responses exist in various WAT depots of different age groups.

Unexpectedly, anti-VEGF treatment caused opposing effects on WAT adipocyte sizes in younger and elder mice. At 1 mo of age, anti-VEGF treatment significantly increased adipocyte diameters in scWAT and epiWAT (Fig. 3 *A* and *D* and Fig. S2 *C* and *E*). Treatment with the same anti-VEGF neutralizing antibody showed significant effects on reduction of adipocyte sizes in 15-mo-old mice (Fig. 3 *A* and *D* and Fig. S2 *C* and *E*). A similar inhibitory effect on adipocyte size by anti-VEGF treatment was seen in 7-mo epiWAT, but not in scWAT (Fig. 3 *A* and *D* and Fig. S2 *C* and *E*). These findings show opposing effects of anti-VEGF treatment on WAT adipocyte sizes in younger and elder mice. Despite the overt changes of WAT adipocyte sizes in different age groups, only modest alterations of body weight, BMI, scWAT, and epiWAT weight were observed in anti-VEGF-treated compared with nontreated mice (Fig. 3 *B* and *C* and Fig. S2*D*).

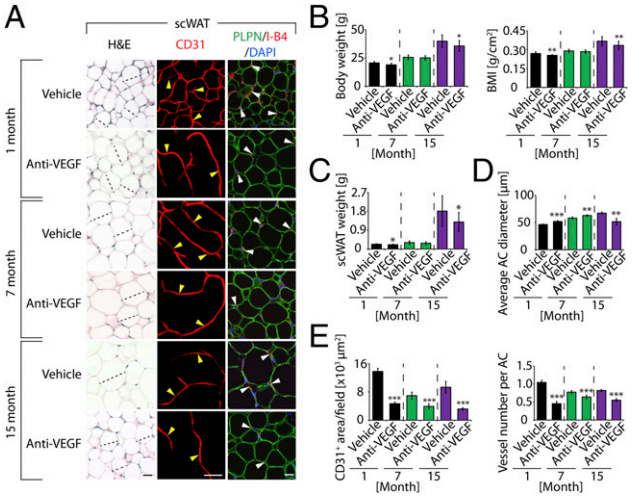

Fig. 3. Anti-VEGF therapy-induced vascular and adipocyte changes in scWAT. (*A*) Histology of adipocytes and vascular density of anti-VEGF– and vehicle-treated scWAT. scWATs were stained with H&E, CD31, or PLPN (blue) plus I-B4 (red) counterstained with DAPI (blue). Arrowheads point to microvessels. Dashed lines show diameters of typical adipocytes. (Scale bars, 50 μm.) (*B*) Body weight and BMI of anti-VEGF– and vehicle-treated 1-, 7-, and 15-mo-old mice (10–18 mice per group). (*C*) Total weight of scWAT of anti-VEGF– and vehicle-treated 1-, 7-, and 15-mo-old mice (n = 10–18). (*D*) Average diameters of anti-VEGF– and vehicle-treated scWAT adipocytes. Adipocyte sizes were quantified from 120 adipocytes from 12 fields. (*E*) Quantification of total microvessel density and numbers per adipocyte in anti-VEGF– and vehicle-treated scWAT (12 fields per group). *P < 0.05, **P < 0.01, ***P < 0.001.

We then studied the effect of anti-VEGF treatment on adipose microvessels and adipocytes in intBAT. Similar to WAT, anti-VEGF treatment also resulted in significant regression of microvessels in intBAT in all age groups (Fig. S3 *A* and *C*), albeit the vascular regressive activity was less robust than in WAT (Fig. 3 *A* and *E* and Fig. S2 *C* and *F*). In response to anti-VEGF treatment, intBAT adipocyte sizes remained virtually unchanged, except for a significant decrease of adipocyte size in the 7-mo group (Fig. S3 *A* and *B*). UCP1 levels in intBAT remained unchanged in all treated groups versus their corresponding control groups (Fig. S3 *A* and *D*).

VEGFR2 Mediates VEGF-Triggered Survival Signaling for Adipose Vasculature. To define receptor-mediated signaling pathways in adipose depots, we treated mice of different ages with anti-VEGFR2 neutralizing antibody (anti-VEGFR2 treatment) (20, 21). Similar to anti-VEGF treatment, anti-VEGFR2 treatment markedly decreased vascular density in scWAT and epiWAT of all age groups (Fig. 4 *A* and *E* and Fig. S4 *A*, *D*, and *E*). No overwhelming effect of anti-VEGFR2 treatment on body weight, BMI, or scWAT and epiWAT weight was observed, merely a subtle decrease in elder mice (Fig. 4 *B* and *C* and Fig. S4*B*). Adipose vasculatures in 7-mo-old scWAT and epiWAT showed intrinsic resistance to anti-VEGFR2 treatment, as seen in anti-VEGF-treated animals (Fig. 3 and Fig. S2*C*). Moreover, virtually identical patterns of anti-VEGF-altered adipocyte sizes in scWAT and epiWAT were reproduced with anti-VEGFR2 treatment. In 1-mo-old mice, anti-VEGFR2 treatment significantly increased adipocyte sizes of WAT while reducing adipocyte sizes in midaged and elder mice (Fig. 4 *A* and *D* and Fig. S4 *A* and *C*).

Anti-VEGFR2 treatment also resulted in significant decreases of vascular density (measured by vessel numbers per adipocyte) in intBAT of 1- and 7-mo-old but not elder mice (Fig. S4 *A* and *E*). Consistent with reduction of vascular density, anti-VEGFR2 treatment significantly inhibited UCP1 expression levels in 1- and 7-mo-old but not in elder mice (Fig. S4 *A* and *F*). These data

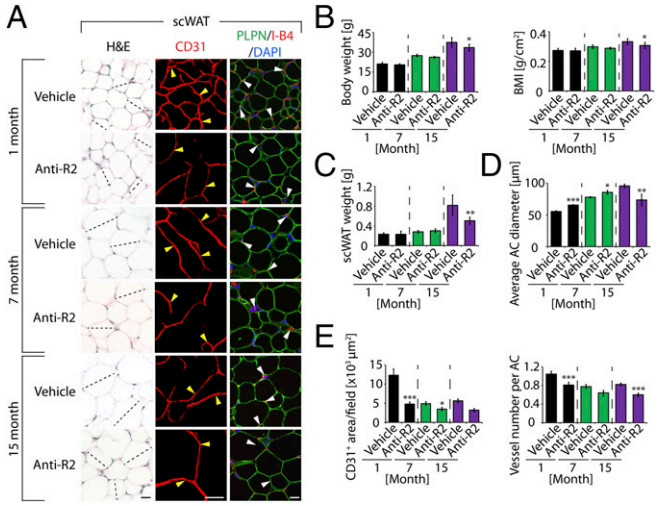

Fig. 4. Anti-VEGFR2 therapy-induced vascular and adipocyte changes in scWAT. (*A*) Histology of adipocytes and vascular density of anti-VEGFR2 (anti-R2)– and vehicle-treated scWAT of different age groups. scWATs were stained with H&E, CD31, or PLPN plus I-B4 (red) counterstained with DAPI (blue). Arrowheads point to microvessels. Dashed lines show diameters of typical adipocytes. (Scale bars, 50 μm.) (*B*) Body weight and BMI of anti-R2– and vehicle-treated 1-, 7-, and 15-mo-old C57BL/6 mice ($n = 10$). (*C*) Total weight of scWAT of anti-R2– and vehicle-treated 1-, 7-, and 15-mo-old mice ($n = 10$). (*D*) Average diameters of anti-R2– and vehicle-treated scWAT adipocytes. Adipocyte sizes were quantified from 120 adipocytes from 12 fields. (*E*) Quantification of total microvessel density and numbers per adipocyte in anti-R2– and vehicle-treated scWAT (12 fields per group). $*P < 0.05$, $**P < 0.01$, $***P < 0.001$.

demonstrate differential responses of intBAT to anti-VEGFR2 treatment between younger and older animals.

Anti-VEGF Improves Insulin Sensitivity in Elder and Obese Mice. We next measured blood lipids in anti-VEGF-treated and nontreated mice. Anti-VEGF treatment significantly increased serum triglyceride and nonesterified fatty acids levels in all groups, whereas glycerol increase was only observed in the 1-mo group (Fig. 5*A*). However, anti-VEGF treatment increased serum cholesterol in 7-mo-old mice (Fig. 5*A*). Under fasting conditions, nontreated mice at 15 mo of age exhibited insulin resistance relative to younger mice (Fig. 5 *B* and *C*). Anti-VEGF treatment significantly reduced fasting insulin and glucose levels and improved insulin sensitivity (Fig. 5 *B* and *C*). In younger mice (1 mo and 7 mo), anti-VEGF treatment also significantly decreased serum glucose levels, although serum insulin levels remained unaffected, leading to improved insulin sensitivity (Fig. 5 *B* and *C*).

To validate the impact of anti-VEGF treatment on insulin sensitivity, we performed an insulin tolerance test. One-month-old and 15-mo-old mice showed significantly increased levels of glucose clearance after anti-VEGF treatment (Fig. 5 *D* and *F*), supporting the finding that inhibition of VEGF increased insulin sensitivity. In contrast, anti-VEGF treatment did not alter glucose clearance in 7-mo-old mice (Fig. 5*E*), indicating that midaged mice were resistant to anti-VEGF-induced insulin sensitivity. These data demonstrate that different age groups responded differentially to anti-VEGF treatment.

Because VEGF has been reported to recruit inflammatory macrophages, it is possible that anti-VEGF treatment would affect inflammatory cells in the adipose tissues. We analyzed inflammatory cells and found that the total population of inflammatory macrophages was not altered in anti-VEGF-treated epiWAT apart from a slight increase in the 15-mo group (Fig. S5 *A* and *B*). Expression of the inflammatory cytokine TNF-α in the epiWAT of anti-VEGF-treated mice was significantly increased in the 15-mo group whose insulin sensitivity was improved by anti-VEGF treatment (Fig. 5 *B*, *C*, and *F* and Fig. S5*C*). Because inflammatory macrophages and cytokines contribute to insulin resistance (2), it is unlikely that increase of macrophages would contribute to anti-VEGF-induced insulin sensitivity. Furthermore, anti-VEGF treatment did not alter microvessel density in the skeletal muscle tissue (Fig. S5*D*), suggesting that it is unlikely that this glucose-uptake organ would be responsible for anti-VEGF-improved insulin sensitivity.

To investigate whether anti-VEGF treatment would improve insulin sensitivity in obese mice, we treated 7-mo-old obese mice fed a high-fat diet (HFD). Anti-VEGF treatment significantly reduced body weight and BMI in HFD-obese mice (Fig. 5*G*). It seemed that body weight loss was due to loss of adipose tissues, because scWAT and epiWAT mass in anti-VEGF-treated obese mice were significantly less than in vehicle-treated control mice (Fig. 5*H*). These findings indicate that inhibition of VEGF prevents HFD-induced obesity development. Anti-VEGF treatment reduced serum insulin and glucose levels, resulting in marked improvement of insulin sensitivity (Fig. 5 *I* and *J*). Similarly, insulin tolerance test showed that anti-VEGF-treated obese mice exhibited markedly increased glucose clearance (Fig. 5*K*), indicating improved insulin sensitivity in HFD-induced obesity. It is unlikely that

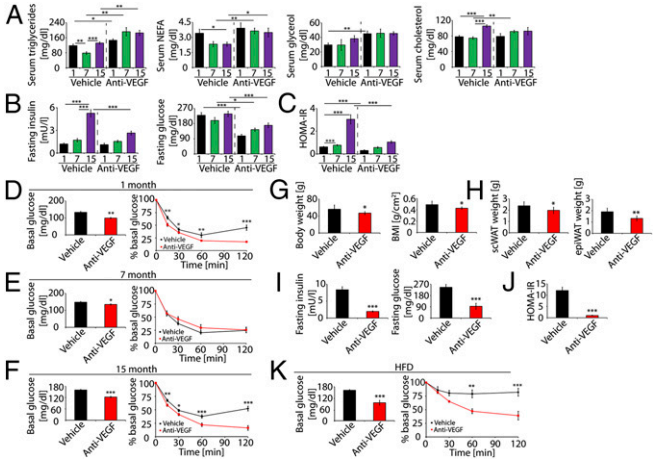

Fig. 5. Anti-VEGF-induced changes of blood lipids, glucose and insulin. (*A*) Serum levels of triglyceride, nonesterified fatty acids (NEFAs), glycerol, and cholesterol in anti-VEGF- and vehicle-treated 1-, 7-, and 15-mo-old mice (10–18 samples in duplicates per group). (*B*) Fasting serum levels of insulin and glucose of anti-VEGF- and vehicle-treated 1-, 7-, and 15-mo-old mice (10–18 samples in duplicates per group). (*C*) Homeostatic model assessment of insulin resistance (HOMA-IR) was calculated using the following formula: serum glucose × serum insulin/22.5. HOMA-IR was calculated based on values presented in *B* (10–18 samples in duplicates per group). (*D*) Insulin tolerance test in vehicle- and anti-VEGF-treated 1-mo-old mice ($n = 10$). Left panel shows basal serum levels of fasting glucose before insulin injection. These basal values were used to normalize the values measured at various time points presented in the right panel. (*E*) Insulin tolerance test in vehicle- and anti-VEGF-treated 7-mo-old mice ($n = 12$). (*Left*) Basal serum levels of fasting glucose before insulin injection. (*Right*) These basal values were used to normalize the values measured at various time points. (*F*) Insulin tolerance test in vehicle- and anti-VEGF-treated 15-mo-old mice ($n = 15$). (*Left*) Basal serum levels of fasting glucose before insulin injection. (*Right*) These basal values were used to normalize the values measured at various time points. (*G*) Body weight and BMI of anti-VEGF- and vehicle-treated HFD-fed mice ($n = 10$). (*H*) Weight of scWAT and epiWAT of vehicle- and anti-VEGF-treated HFD-fed mice ($n = 10$). (*I*) Fasting serum levels of insulin and glucose of anti-VEGF- and vehicle-treated HFD-fed mice (10 samples in duplicates per group). (*J*) HOMA-IR was calculated based on values presented in *B* (10 samples in duplicates per group). (*K*) Insulin tolerance test of vehicle- and anti-VEGF-treated HFD-fed mice. $*P < 0.05$, $**P < 0.01$, $***P < 0.001$.

MEDICAL SCIENCES

alterations of inflammatory macrophages in anti-VEGF-treated WAT are responsible for improvement of insulin sensitivity because macrophage numbers in epiWAT of treated obese mice were not significantly altered (Fig. S5 *A* and *B*). Inflammatory cytokines including IL-6 and TNF-α were significantly increased in anti-VEGF-treated epiWAT of HFD-fed obese mice (Fig. S5*C*). Consistent with improvement of insulin sensitivity, adipocyte sizes of scWAT and epiWAT were significantly smaller in anti-VEGF-treated mice (Fig. 6 *B* and *C*). Interestingly, VEGF levels were nearly identical in scWAT and epiWAT of HFD-fed mice (Fig. 6*A*). Adipose microvessel density was significantly reduced in anti-VEGF treated HFD-fed mice (Fig. 6 *B*, *D*, and *E*). Of note, anti-VEGF treatment induced vascular regression in epiWAT of HFD-fed animals (Fig. 6*E*). These findings imply that obese individuals may potentially benefit more from anti-VEGF therapy because visceral WAT is primarily linked to development of type 2 diabetes and cardiovascular disease.

In HFD-fed mice, intBAT revealed high contents of lipid droplets, leading to increased adipocyte sizes (Fig. S6*A*). Anti-VEGF treatment significantly reduced intBAT weight, adipocyte size, and lipid droplets while increasing the mitochondrial content (Fig. S6 *A*, *B*, and *D*). Similar to WATs, blocking VEGF inhibited intBAT vascularization in HFD-fed mice (Fig. S6 *A* and *C*). Expression of *Ucp1* mRNA in anti-VEGF-treated and nontreated intBAT remained at similar levels (Fig. S6 *A* and *E*).

Discussion

Here we have reported VEGF-dependent vascular plasticity in WATs and BAT during aging. VEGF expression in adipose depots varies in different age groups, which show significant differences in anti-VEGF sensitivity. Anti-VEGF treatment produces opposing effects on WAT adipocyte sizes in younger and elder mice, leading to marked differences in insulin sensitivity. Surprisingly, HFD-fed obese mice are more likely to develop VEGF-dependent insulin resistance, and anti-VEGF therapy significantly improves insulin sensitivity. Our results may provide valuable information for the treatment of type 2 diabetes with antiangiogenic drugs and imply that different age populations and their BMI status may affect therapeutic outcomes. Adipose tissue, especially WAT, is probably the most unique tissue in our body, continuously undergoing expansion and shrinkage. This plasticity would inevitably alter cellular and molecular components in the adipose microenvironment. Other cell components including endothelial, perivascular, inflammatory, and mesenchymal cells also constantly change their numbers and functions to cope with the metabolic demand of adipocytes. This is particularly true in adult and aged populations. Among all nonadipocyte components, blood vessels are the most dominant structures (22–24), displaying tremendous plasticity. Pharmacological inhibition of adipose angiogenesis in obese animals demonstrated beneficial effects in preventing obesity development (25–27).

Recent studies using genetic mouse models have investigated the role of VEGF in obesity and insulin sensitivity. In gain-of-function experiments, overexpression, rather than inhibition, of VEGF in adipose tissues protects diet-induced obesity and insulin resistance (12, 28, 29). However, temporary systemic loss of VEGF function in mice also results in a lean phenotype and improvement of insulin sensitivity (30). Despite these discrepancies, the age-related issue has not been carefully studied. In our study, we demonstrate that inhibition of VEGF significantly increases adipocyte sizes in younger mice, but opposite effects can be seen in midaged and elder mice. Anti-VEGF-induced polarized effects seem to be mediated by VEGFR2 signaling because anti-VEGFR2 treatment reproduces the opposing effects on adipocyte sizes. Because VEGFR2 expression is relatively restricted to vascular endothelial cells (31), recapitulation of anti-VEGF effects by the anti-VEGFR2 treatment demonstrates that the vasculature is primarily responsible for adipocyte alterations. Enlargement of adipocytes by anti-VEGF treatment has not been translated into increased body weight and BMI in these younger mice. Perhaps continuous development of nonadipose tissues and organs affect the total body weight in these mice. However, decreases of adipocyte sizes in anti-VEGF-treated midaged mice do not result in significantly reduced body weight and BMI, whereas reduced body weight and BMI was observed in anti-VEGF-treated elder animals.

We cannot exclude possibilities that nonadipose tissues are also involved in modulation of anti-VEGF-improved insulin sensitivity. Our recent study showed that systemic treatment of healthy mice (8–12 wk old) resulted in vascular reduction in several endocrine organs including pancreas, adrenal gland, and thyroid (20). Despite anti-VEGF-induced vascular reduction in pancreas, circulating insulin levels remained unaltered, suggesting that insulin production is less likely the mechanism for anti-VEGF-improved sensitivity. The insulin tolerance test further supports this view because anti-VEGF treatment significantly improved glucose clearance, suggesting modulation of insulin utilization rather than production as the mechanism. Skeletal muscle tissue is the largest organ for glucose uptake; however, we have found that anti-VEGF treatment did not affect microvessel density in this tissue. Thus, it is unlikely that the effect of anti-VEGF treatment on skeletal muscle tissues would have a significant impact on insulin sensitivity in our model system.

One of the most interesting findings is that anti-VEGF treatment markedly reduces blood glucose levels. These findings are significant and imply that systemic delivery of anti-VEGF drugs would be likely to alter glucose levels in humans. In fact, anti-VEGF drugs including bevacizumab, aflibercept, and many tyrosine kinase inhibitors are now routinely used for treatment of human cancers (16). It would be interesting to investigate in cancer patients whether anti-VEGF drugs significantly alter blood glucose levels. Because malignant cells primarily use the glycolytic pathway (Warburg effect) for their growth, decreases of blood

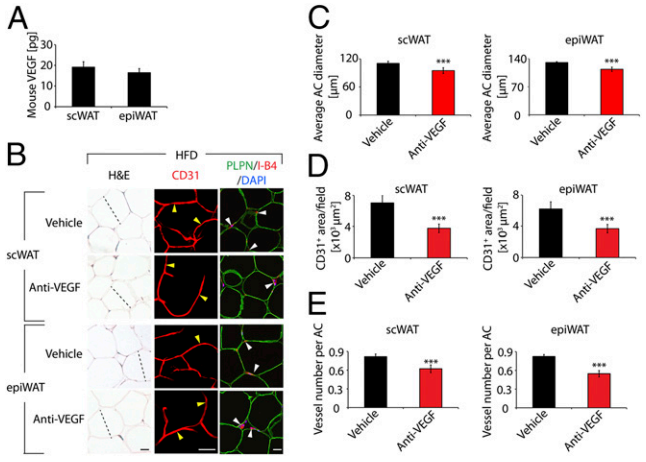

Fig. 6. VEGF levels and anti-VEGF therapy-induced vascular and adipocyte changes in healthy and obese WATs. (*A*) Quantification of VEGF protein levels in scWAT and epiWAT of HFD-fed mice (four samples in duplicates per group). (*B*) Histology adipocytes and vascular density of anti-VEGF- and vehicle-treated scWAT and epiWAT of HFD-fed mice. WATs were stained with H&E, CD31, or PLPN (green) plus I- B4 (red) counterstained with DAPI (blue) nucleus staining. Arrowheads point to microvessels. Dashed lines show diameters of typical adipocytes. (Scale bars, 50 μm.) (*C*) Average diameters of anti-VEGF- and vehicle-treated scWAT and epiWAT adipocytes of HFD-fed mice. Adipocyte sizes were quantified from 120 adipocytes from 12 fields. (*D*) Quantification of total microvessel density in anti-VEGF- and vehicle-treated scWAT and epiWAT (12 fields per group). (*E*) Quantification of microvessel numbers per adipocyte in anti-VEGF- and vehicle-treated scWAT and epiWAT. ***$P < 0.001$.

glucose levels by anti-VEGF drugs would offer an attractive mechanism of action. However, antiangiogenic drugs are often given to cancer patients in combination with chemotherapeutics, which significantly affect metabolic parameters in human patients. Thus, it would be difficult to study the putative effect of anti-VEGF drugs in humans. In elder mice that are resistant to insulin, anti-VEGF treatment significantly improves insulin sensitivity. However, this significant effect is absent in midaged mice. It would be reasonable to speculate that elder populations would potentially have greater benefits from anti-VEGF treatment regarding insulin sensitivity. We should emphasize that some value changes in our experimental settings—although statistically significant—show a relatively small magnitude of alteration. However, subtle changes of VEGF signaling molecules and vessel density could potentially lead to robust physiological or pathological changes owing to threshold regulatory mechanisms. This interesting phenomenon warrants further investigation.

We chose a diet-induced obesity model to study the effect of anti-VEGF drugs on adipose vasculatures, adipocytes, and insulin sensitivity because diet-induced obesity is the most common cause of obesity in humans (32, 33). Our findings show that VEGF is the primary factor for maintenance of vascular networks in obese WAT and inhibition of VEGF leads to regression of most microvessels in both s.c. and epididymal WATs. Unexpectedly, anti-VEGF treatment produces a more robust effect in improvement of insulin sensitivity in obese mice compared with healthy mice. In HFD-fed animals, total weight of intBAT is also significantly increased and enlargement of BAT in obese mice reflects the fact of excessive energy storage in this otherwise energy-expending organ. Interestingly, anti-VEGF treatment markedly reduces the total volume of intBAT in HFD-induced obese animals owing to inhibition of lipid deposition in this tissue. In healthy mice, anti-VEGF and anti-VEGFR2 treatment produce differential effects on intBAT activation in younger and midaged mice. Whereas anti-VEGF treatment does not affect intBAT-*Ucp1* expression at any age, anti-VEGFR2 treatment significantly inhibits intBAT-*Ucp1* expression in younger and midaged mice. We have recently shown in cold-exposed animals that anti-VEGFR1 and anti-VEGFR2 treatment result in opposing effects on cold-induced UCP1-dependent nonshivering thermogenesis (11). Anti-VEGF therapy would indistinguishably block signaling pathways triggered by VEGFR1 and VEGFR2 and would impair both receptor-mediated opposing effects on UCP1-dependent nonshivering thermogenesis. Thus, it is perhaps not surprising to observe differential effects on UCP1 expression in response to anti-VEGF and anti-VEGFR2 treatments. However, it is unknown why elder mice did not show differential responses to anti-VEGF or anti-VEGFR2 treatment.

If our findings can be successfully translated into clinical settings, anti-VEGF agents could be potentially useful for treatment of type 2 diabetes, which frequently occurs in obese human individuals. Taken together, our findings, for the first time to our knowledge, demonstrate that adipose vasculatures in adulthood exhibit plasticity and VEGF is a crucial vascular maintenance factor at all ages. These data provide valuable information for therapeutic intervention of obesity and diabetes by targeting the adipose vasculature.

Materials and Methods

Animals. All animal studies were approved by the North Stockholm Animal Ethics Committee. C57BL/6 female mice at ages of 1, 4, 7, 10, 12, 15, and 16 mo were maintained under standard animal housing conditions at 22 °C and received either normal chow or HFD (Research Diets). See details in *SI Materials and Methods*.

ACKNOWLEDGMENTS. The Y.C. laboratory is supported by the Swedish Research Council, the Swedish Cancer Foundation, the Karolinska Institute Foundation, the Karolinska Institute Distinguished Professor Award, Torsten Söderbergs Foundation, the Novo Nordisk Foundation, and European Research Council Advanced Grant ANGIOFAT (Project 250021).

1. Facchini FS, Hua N, Abbasi F, Reaven GM (2001) Insulin resistance as a predictor of age-related diseases. *J Clin Endocrinol Metab* 86(8):3574–3578.
2. Johnson AM, Olefsky JM (2013) The origins and drivers of insulin resistance. *Cell* 152(4):673–684.
3. Powell K (2007) Obesity: The two faces of fat. *Nature* 447(7144):525–527.
4. Després JP, Lemieux I (2006) Abdominal obesity and metabolic syndrome. *Nature* 444(7121):881–887.
5. Cao Y (2010) Adipose tissue angiogenesis as a therapeutic target for obesity and metabolic diseases. *Nat Rev Drug Discov* 9(2):107–115.
6. Cao Y (2013) Angiogenesis and vascular functions in modulation of obesity, adipose metabolism, and insulin sensitivity. *Cell Metab* 18(4):478–489.
7. Cao Y (2007) Angiogenesis modulates adipogenesis and obesity. *J Clin Invest* 117(9): 2362–2368.
8. Tang W, et al. (2008) White fat progenitor cells reside in the adipose vasculature. *Science* 322(5901):583–586.
9. Gupta RK, et al. (2012) Zfp423 expression identifies committed preadipocytes and localizes to adipose endothelial and perivascular cells. *Cell Metab* 15(2):230–239.
10. Tran KV, et al. (2012) The vascular endothelium of the adipose tissue gives rise to both white and brown fat cells. *Cell Metab* 15(2):222–229.
11. Xue Y, et al. (2009) Hypoxia-independent angiogenesis in adipose tissues during cold acclimation. *Cell Metab* 9(1):99–109.
12. Sung HK, et al. (2013) Adipose vascular endothelial growth factor regulates metabolic homeostasis through angiogenesis. *Cell Metab* 17(1):61–72.
13. Ferrara N, Kerbel RS (2005) Angiogenesis as a therapeutic target. *Nature* 438(7070): 967–974.
14. Cao Y (2009) Positive and negative modulation of angiogenesis by VEGFR1 ligands. *Sci Signal* 2(59):re1.
15. Alon T, et al. (1995) Vascular endothelial growth factor acts as a survival factor for newly formed retinal vessels and has implications for retinopathy of prematurity. *Nat Med* 1(10):1024–1028.
16. Cao Y, et al. (2011) Forty-year journey of angiogenesis translational research. *Sci Transl Med* 3:114rv113.
17. Cao Y, Langer R (2010) Optimizing the delivery of cancer drugs that block angiogenesis. *Sci Transl Med* 2(15):ps3.
18. Kerbel RS (2008) Tumor angiogenesis. *N Engl J Med* 358(19):2039–2049.
19. Yang X, et al. (2013) Vascular endothelial growth factor-dependent spatiotemporal dual roles of placental growth factor in modulation of angiogenesis and tumor growth. *Proc Natl Acad Sci USA* 110(34):13932–13937.
20. Yang Y, et al. (2013) Anti-VEGF- and anti-VEGF receptor-induced vascular alteration in mouse healthy tissues. *Proc Natl Acad Sci USA* 110(29):12018–12023.
21. Xue Y, et al. (2008) Anti-VEGF agents confer survival advantages to tumor-bearing mice by improving cancer-associated systemic syndrome. *Proc Natl Acad Sci USA* 105(47): 18513–18518.
22. Cao Y (2014) Angiogenesis as a therapeutic target for obesity and metabolic diseases. *Chem Immunol Allergy* 99:170–179.
23. Lim S, et al. (2012) Cold-induced activation of brown adipose tissue and adipose angiogenesis in mice. *Nat Protoc* 7(3):606–615.
24. Xue Y, Lim S, Bråkenhielm E, Cao Y (2010) Adipose angiogenesis: Quantitative methods to study microvessel growth, regression and remodeling in vivo. *Nat Protoc* 5(5):912–920.
25. Kim YM, et al. (2007) Assessment of the anti-obesity effects of the TNP-470 analog, CKD-732. *J Mol Endocrinol* 38(4):455–465.
26. Bråkenhielm E, et al. (2004) Angiogenesis inhibitor, TNP-470, prevents diet-induced and genetic obesity in mice. *Circ Res* 94(12):1579–1588.
27. Rupnick MA, et al. (2002) Adipose tissue mass can be regulated through the vasculature. *Proc Natl Acad Sci USA* 99(16):10730–10735.
28. Elias I, et al. (2012) Adipose tissue overexpression of vascular endothelial growth factor protects against diet-induced obesity and insulin resistance. *Diabetes* 61(7): 1801–1813.
29. Sun K, et al. (2012) Dichotomous effects of VEGF-A on adipose tissue dysfunction. *Proc Natl Acad Sci USA* 109(15):5874–5879.
30. Lu X, et al. (2012) Resistance to obesity by repression of VEGF gene expression through induction of brown-like adipocyte differentiation. *Endocrinology* 153(7):3123–3132.
31. Ferrara N, et al. (1996) Heterozygous embryonic lethality induced by targeted inactivation of the VEGF gene. *Nature* 380(6573):439–442.
32. Rosenbaum M, Leibel RL, Hirsch J (1997) Obesity. *N Engl J Med* 337(6):396–407.
33. Hill JO, Peters JC (1998) Environmental contributions to the obesity epidemic. *Science* 280(5368):1371–1374.